Experimental analysis of mode coupling and plasma turbulence induced by magnetic fields

A. A. Ferreira, M. V. A. P. Heller, and I. L. Caldas
Institute of Physics, University of São Paulo, C. P. 66318, 05315-970 São Paulo, SP, Brazil

(Received 11 January 2000; accepted 16 May 2000)

Wavelet spectrum and bispectrum techniques are applied to study the development of temporal turbulence induced by a confinement toroidal magnetic field in a toroidal magnetoplasma created by radio frequency waves. For low magnetic fields the plasma is roughly uniform and the analyzed electrostatic linear frequency spectra are essentially determined by the driven radio frequencies. However, by increasing the toroidal magnetic field, gradients in the plasma radial profiles and broader frequency spectra are observed. Thus, spectral components with frequencies higher than those injected in the plasma are excited. Moreover, this variation of magnetic field also induces nonlinear phase coupling between low frequency coherent peaks and continuous high frequency spectral components. © *2000 American Institute of Physics.* [S1070-664X(00)00709-6]

I. INTRODUCTION

The interest in plasma-edge turbulence in confinement devices is based on the evidence that improvements of plasma confinement depend on the plasma edge behavior.[1,2] Remarkably, experiments show that anomalous edge particle transport is induced by electrostatic turbulence. Thus, identifying the main characteristics of this turbulence is important, as its spectra and driven sources.

Interactions and couplings between excited fluctuations can lead to turbulence and turbulent fluctuations can be interpreted as nonlinear wave–wave interactions of unstable drift modes.[3] Therefore, a purely linear analysis is unable to explain how electrostatic waves, initially unstable in a limited frequency range, can generate a turbulent spectrum extended over a broader range of frequencies. Thus, nonlinear wave interactions have been investigated by performing bispectral analyses. This procedure reveals several important fluctuation couplings in the presence of turbulence, but few investigations have dealt directly with the onset of turbulence.

Experimental work, carried out on a linear device, showed that drift waves may destabilize, depending on the ion gyroradius, and generate a turbulent spectrum.[4] Another experimental investigation showed that turbulence develops in a toroidal magnetoplasma due to drift wave destabilization by a large magnetic confinement field.[5] In this last reference, bispectral analyses revealed that nonlinear couplings may play an important role in the development of turbulence. However, with the performed spectral analysis, identifying primary modes that were responsible for the generation of other frequencies was not possible. On the other hand, in another experiment[6] in a toroidal device without plasma current, anomalous transport was associated to intermittent large coherent vortical structures. Although drift wave instability may coexist with flute modes, the observed coherent structures are of the flute type.

In this experiment we investigate, in a toroidal magnetoplasma (without plasma current) created by radio frequency waves, the development of temporal turbulence induced by increasing the confinement toroidal magnetic field. For a complete characterization of plasma turbulence, we measured density and potential fluctuations and their phases and correlation.[7,8] Thus, for the present investigation, we projected and installed at Tokamak Chauffage Alfvén-Brazil (TCABR) a system of probes, that measures simultaneously electrostatic fluctuation and some plasma mean parameters. Furthermore, the obtained data were treated with wavelet spectral and bispectral estimating methods[3,9,10] to determine linear and quadratic couplings between the measured fluctuations. The wavelet analysis is adopted because the onset of turbulence may be related to nonstationary intermittent oscillations as those observed in Ref. 6.

For the low magnetic field, we observe that plasma density and temperature profiles are roughly uniform while analyzed electrostatic linear frequency spectra are essentially determined by the driven radio frequency. However, increasing the toroidal magnetic field, the confinement improves and we observe gradients in the plasma profiles. Then, spectral components, with frequencies higher than those injected in the plasma, are excited generating broader continuous frequency spectra that indicate the onset of turbulence. Moreover, the magnetic field enhancement also induces nonlinear phase coupling between low frequency coherent peaks and high frequency noncoherent spectral components. Therefore, the reported turbulence onset caused by nonlinear couplings may contribute to identifying the nature of instabilities and the basic mechanisms determining edge turbulence.[11,12]

The outline of this paper is as follows: In Sec. II we give a brief description of the apparatus and basic spectral analysis techniques. In Sec. III A, we describe the behavior of density, plasma potential equilibrium, and fluctuation profiles. In Sec. III B we analyze the spectral and bispectral characteristics of the electrostatic turbulence. In Sec. IV we summarize the conclusions of this work.

II. APPARATUS AND TECHNIQUES OF ANALYSIS

The experiment is performed with a hydrogen magnetized circular plasma in the toroidal device of the TCABR tokamak (major radius $R_0=0.610$ m and minor radius $a=0.175$ m),[13] using its facilities available for cleaning discharges. The stationary plasma is obtained by a (16 kHz) radio frequency oscillator with a pulse length of 25 ms. Hydrogen pressure is 10^{-4} Pa. Typically obtained plasma edge parameters are $T_e<30$ eV and $n<5\times10^{16}\,\mathrm{m}^{-3}$. To study the turbulence onset we apply two different toroidal magnetic fields, namely, $B_\varphi=0.04$ T and 1.00 T. There is no induced toroidal electric field and no externally imposed toroidal electric current. Consequently, there is no poloidal magnetic field.

The data were collected from a multipin Langmuir probe, inserted into the plasma through a diagnostic port, toroidally displaced far from the poloidal limiter. The probe system is mounted on a four bellow-operated shafts, with a total excursion of 30×10^{-2} m. This probe system was composed by four tungsten cylindrical tips 5×10^{-3} m long and 0.6×10^{-3} m diameter. Two of the four pin configuration measures the floating potential fluctuations, $\tilde{V}_f$, another measures the ion saturation current fluctuations, $\tilde{I}_{si}$, and the other is used in the sweep mode to determine mean density, electron temperature and plasma potential. Neglecting the temperature fluctuations the probes measure the plasma potential and the electron density.

The study of turbulence is based on digital correlation techniques applied to floating potential fluctuations and ion saturation current fluctuations. The time series measurements are recorded using an Analogic Digital Converter (ADC) in a Versa Module Eurocard (VME) board with 12 bit digitizers, with a maximum sampling rate of 1 Mhz.

To examine the time behavior of the fluctuations we split the data into eight consecutive segments of 1024 data points ($\approx$1.02 ms) and we apply the wavelet analysis to each segment. We use wavelet analysis,[9,14–16] which permits time resolution of short interval data, convenient to investigate any possible intermittent fluctuation during each single discharge. The application is based on a wavelet function set that changes its size and position by dilatation and shifting. Thus, the wavelets transform decomposes the experimental time series using a wavelet basis of functions localized both in time and frequency domains.

In this analysis we used the continuous wavelet transform based on the Morlet wavelet:[16]

$$\Psi_\alpha(t)=\alpha^{-1/2}\exp[i2\pi t/\alpha-(t/\alpha)^2/2]. \tag{1}$$

A frequency $f=2\pi/\alpha$ is assigned to each scale α. The frequency resolution of the wavelet $\Psi_\alpha(t)$ is $\Delta f=f/4$, and the time resolution is $\Delta t=2\alpha$. If $x(t)$ is the signal under analysis, the wavelet transform of $x(t)$ with respect to a chosen mother wavelet $\Psi_\alpha(t)$ is defined by Ref. 16:

$$W_x(\alpha,\tau)=\int x(t)\Psi_\alpha(t-\tau)dt, \tag{2}$$

where α is a scaling parameter and τ is a time shift parameter.

We define the cross-power spectrum for two time series $x(t)$ and $y(t)$:

$$C_{yx}(\alpha,T)=\int_T W_x(\alpha,\tau)W_y^*(\alpha,\tau)d\tau. \tag{3}$$

To quantify where two nonstationary fluctuating signals are linearly correlated at a particular scale (frequency) and time location in a time-scale plane, we defined the coherence spectrum with values in the interval $0\leqslant\gamma_{xy}^2\leqslant1$. When there is a perfect linear relation at some frequency it is equal to 1. Accordingly, the coherence spectrum was defined as

$$\gamma_{yx}^2(\alpha,T)=|C_{yx}(\alpha,T)|^2/C_{xx}(\alpha,T)C_{yy}(\alpha,T), \tag{4}$$

where C_{xx} and C_{yy} are the wavelet autopower spectra of the signal's $x(t)$ and $y(t)$, respectively.

We applied the technique of an $S(k,f)$ spectrum[17] using wavelet auto and cross spectra and calculated $S(f)$ and $S(k)$ spectra.

To detect evidence of phase coupling between wavelet components of different scale lengths, possibly present in turbulence,[14,16] we combined wavelet and bispectral analysis by calculating wavelet bispectra and bicoherences between two frequencies and their sum and difference frequencies.

Bicoherence was calculated according to the following definitions. First, the wavelet bispectrum is

$$B(\alpha_1,\alpha_2)=\int_T W_x^*(\alpha,\tau)W_x(\alpha_1,\tau)W_x(\alpha_2,\tau)d\tau, \tag{5}$$

where the integral is taken over a finite interval T as with the linear-wavelet spectrum. The wavelet-bispectrum measures the amount of phase coupling that occurs between wavelet components of scale lengths α_1, α_2 and α such that the sum rule $1/\alpha=1/\alpha_1+1/\alpha_2$, is satisfied. Since the scale lengths may be interpreted as inverse frequencies, the wavelet bispectrum may be interpreted as the coupling of wavelets of frequencies such that $f=f_1+f_2$. Then, the wavelet-bicoherence, substituting the scale lengths by the frequencies, is given by

$$[b(f_1,f_2)]^2=|B(f_1,f_2)|^2\Big/\left[\int_W|(f_1,\tau)W(f_2,\tau)|^2d\tau\right]\times\left[\int_W|(f,\tau)|^2d\tau\right]. \tag{6}$$

The wavelet-bicoherence is usually plotted in the (f_1,f_2) plane. Representing the whole plane is not necessary, because f_1, f_2 and their sum f must be smaller than the Nyquist frequency, and f_1 and f_2 are interchangeable, the plot can be restricted to $f_1\geqslant f_2$ and finally the case (f_1,f_2) is identical to the case $(-f_1,-f_2)$.

A statistical noise level can be associated to wavelet-bicoherence in the same way as Ref. 16,

$$\epsilon[b(f_1,f_2)]=\{(f_N)/N\min(|f_1|,|f_2|,|f|)\}^{1/2}, \tag{7}$$

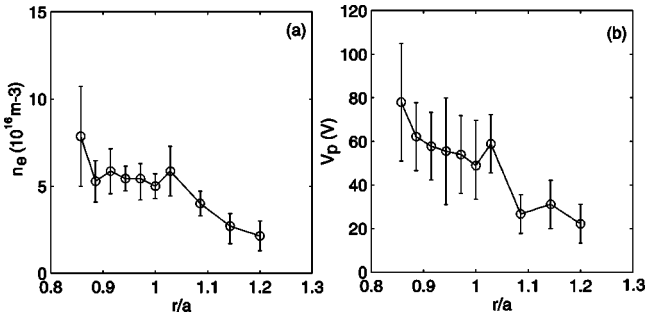

FIG. 1. Density radial profile for the magnetic field of 1.00 T (a); the same for plasma potential (b).

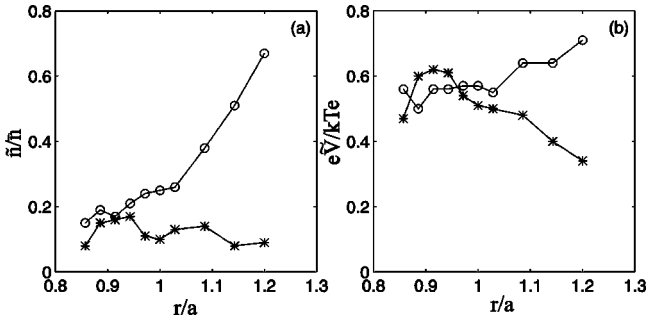

FIG. 2. Normalized radial profiles for density fluctuations and magnetic fields of 0.04 T (*) or 1.00 T (○) (a); the same for normalized plasma potential fluctuations (b).

where N is the number of points and f_N is the Nyquist frequency.

We introduce the summed bicoherence, defined as

$$[b(f)]^2=[1/s(f)]\Sigma[b(f_1,f_2)]^2, \tag{8}$$

where the sum is taken over all f_1 and f_2 such that the summation rule is satisfied, and $s(f)$ is the number of terms of each f, we can obtain the total-bicoherence as

$$(b)^2=(1/S)\Sigma\Sigma[b(f_1,f_2)]^2, \tag{9}$$

where the sum is taken over all f_1 and f_2, and S is the number of terms in the summation. The numerical values of the summed and total-bicoherences depend on the chosen calculation grid, our frequency grid is of 256 points from 0 to 1 MHz, with a frequency cell of 3.9 kHz. As wavelet analysis can be done with short data sequences, we can verify the alterations of total-bicoherence during a discharge time, identifying intermittent behavior.

III. EXPERIMENTAL RESULTS

A. Equilibrium and fluctuation profiles

In this work, to emphasize the influence of the confining magnetic field on the turbulence onset, we present typical plasma equilibrium and fluctuation radial profiles for two toroidal magnetic fields, $B_\varphi=0.04$ T and $B_\varphi=1.00$ T.

Electron temperature, density and plasma potential are estimated by means of Langmuir characteristic curves obtained by using a probe in the sweep mode. Figure 1(a) shows a typical density radial profile for the highest magnetic field. This profile presents a noticeable gradient at the scrape-off-layer (SOL) and is nearly uniform at the plasma edge. In contrast, for the lowest magnetic field, the density profile is flat in both regions. On the other hand, the potential profile [for the same conditions of Fig. 1(a)] is shown in Fig. 1(b). The gradient on the plasma potential, observed in this figure, corresponds to an electric field roughly $E\sim 1\times 10^3$ V/m, in contrast to the low value observed for the other discharges with the lowest magnetic field. This electric field may produce a poloidal plasma rotation affecting stability conditions.[1]

Density and temperature for the magnetic field of 1 T are $n\approx(2-7)\times 10^{16}\,\mathrm{m}^{-3}$ and $T_e\approx(12-30)$ eV. In the scrape-off-layer, the radial decay coefficients are $\lambda_n=-n/\nabla n\approx 2.9\times 10^{-2}$ m, for density, and $\lambda_{Te}=-T_e/\nabla T_e\approx 4.0\times 10^{-2}$ m for electron temperature.

Figure 2 shows normalized fluctuating density (a) and potential (b) profiles for the two applied magnetic fields. Both fluctuations increase with the magnetic field, especially at the scrape-off-layer where the equilibrium gradients are higher. At the plasma edge, relative fluctuation values for plasma potential are higher than for density fluctuations; we find $e\tilde{V}/kT_e\approx 2-3(\tilde{n}/n)$. These values disagree with the adiabatic condition usually assumed to describe drift instabilities that may originate the observed fluctuations. The phase angle between V and $\tilde{n}$ is $\approx\pi/2$ for 1.00 T, as predicted for drift waves, but is $\approx\pi/6$ for the magnetic field of 0.04 T.

For 1.00 T, the radial diffusion coefficient, D, associated with the enhanced density fluctuations, is calculated from the expression[18] $D\approx 2\pi\Delta f(\lambda_n\tilde{n}/n)^2\approx 6\ \mathrm{m}^2/\mathrm{s}$, used for high coherent fluctuations with a phase angle of $\pi/2$. This value is comparable with that obtained for Bohm diffusion $D_B\approx T_e/(16B_\varphi)\approx 1\ \mathrm{m}^2/\mathrm{s}$.

B. Onset of turbulence

Initially, we present wavelet power spectra of the measured fluctuations, for the two different toroidal magnetic fields, $B_\varphi=0.04$ T and $B_\varphi=1.00$ T, at a given radial position. The spectra analyzed for ten different radial positions have the same main characteristics. Calculations are done on the samples after high-pass digital filtering with a cutoff frequency of 1.5 kHz.

Figure 3 shows frequency power spectra of ion saturation current fluctuations (a) and floating potential fluctuations (b), for a time interval of 1.02 ms at $r/a=0.85$ and magnetic fields of 0.04 T or 1.00 T. The frequency spectra are broad and extend up to 60 kHz. The low frequency prominent peak, corresponding to the energy transmitted by the radio frequency oscillator, does not depend on the applied magnetic field, whereas for the continuous high frequency spectra the fluctuation level increases with the magnetic field. The main characteristics of these spectra, obtained for the mentioned time interval, do not change during a pulse.

The enhancement of high frequency components for the 1.00 T field is also identified in Fig. 4 that shows the time

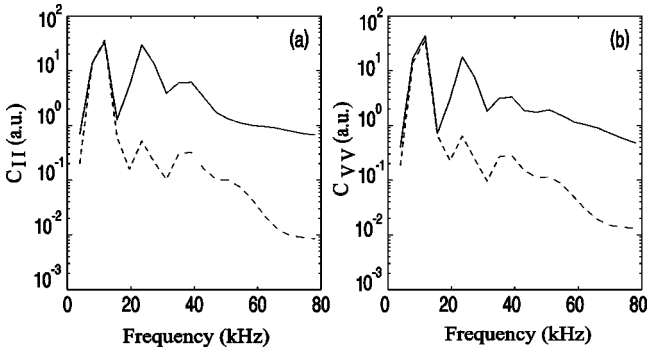

FIG. 3. Frequency power spectra for ion saturation current fluctuations, for magnetic fields of 0.04 T (- - - -) or 1.00 T (——), for a time interval of 1.02 ms at $r/a=0.85$ (a). The same for floating potential fluctuations (b).

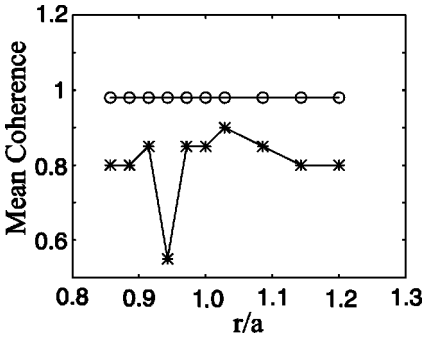

FIG. 5. The mean coherence radial profile between potential and ion saturation current fluctuations for the magnetic field of 0.04 T (*) and 1.00 T (○), respectively.

resolved contour plot of the wavelet spectrum (during a single discharge) for potential fluctuations at $r/a=0.85$ for the magnetic field of 0.04 T (a) or for 1.00 T (b).

Figure 5 shows radial profiles of the mean coherence between potential and ion saturation current fluctuations corresponding to the prominent peaks in the spectrum range of 20–40 kHz (excluding the radio frequency driving peak), for the two applied fields. In this frequency range, coherence is high and frequency independent for both fields. Therefore, this high linear coherence suggests that potential and density fluctuations have the same driving energy sources. Besides, we also estimate from the phase angle spectra, for the prominent coherent peaks, average poloidal wave numbers $k\approx 2\times 10^2\,\mathrm{m}^{-1}$ (for $B_\varphi=0.04\,\mathrm{T}$) and $k\approx 6\times 10^2\,\mathrm{m}^{-1}$ (for $B_\varphi=1.00\,\mathrm{T}$). Therefore, the wave number increases with the magnetic field as expected for drift waves.[1] We estimate also the relevant parameter for the drift wave like turbulence $b=k\rho\approx 2$ (for $B_\varphi=0.04\,\mathrm{T}$) and $b\approx 4\times 10^{-1}$ (for $B_\varphi=1.00\,\mathrm{T}$), where ρ is the ion gyroradius at the electron temperature, obtaining values compatible with those that appear in the drift wave literature.[1,4]

To study the transition to turbulence in the obtained toroidal magnetoplasma, we use wavelet-bispectra[14,16,19] to identify evidence of quadratic interactions between the measured fluctuations (for the two applied magnetic fields). To examine how these interactions are spread in frequencies, we estimated the wavelet bicoherence, the summed, and the total wavelet-bicoherence for eight selected intervals of 1.02 ms during the plasma pulse.

The results for the third interval and $r/a=0.85$ are in Figs. 6(a) and 6(b). These figures show the superposition of the summed bicoherence for the two applied fields for ion saturation current fluctuations (a) and potential fluctuations, (b). For 1 T, nonlinear interactions are more significant for potential than for density fluctuations. The coupling in higher frequencies appears only for the highest confinement field. As shown in this figure, the summed bicoherence values are significantly above the statistical uncertainty.[14]

During a single discharge, the calculated total bicoherence for the two applied fields changes with time. For density fluctuations (calculated at $r/a=0.85$) the total bicoherence, shown in Fig. 7(a), is similar for the two fields with pronounced time dependence only in the initial times. Figure 7(b) shows the superposition of the total bicoherence for the potential fluctuations. In this case, we observe a pronounced time dependence only for 0.04 T. For potential fluctuations and a high magnetic field the total bicoherence values do not depend on the radial position.

Higher frequencies are responsible for the increase of bicoherence. An example of this effect can be observed in Fig. 8, where we calculated the summed bicoherence for density fluctuations at $r/a=1.00$, $B_\varphi=1.00\,\mathrm{T}$, for two intervals in the beginning (a) and the end of a discharge (b). In the last interval the increase of the quadratic coupling is due

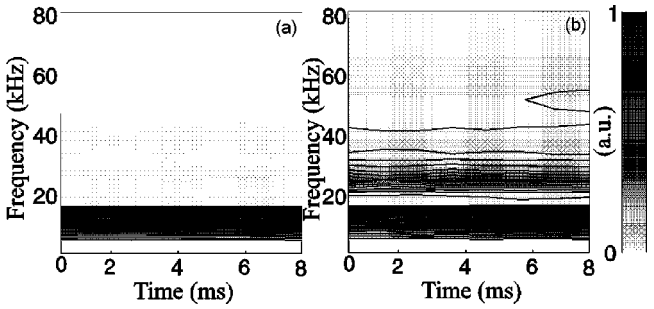

FIG. 4. Time resolved contour plot of the wavelet spectrum for potential fluctuations at $r/a=0.85$ for the magnetic field of 0.04 T (a); the same for the magnetic field of 1.00 T (b).

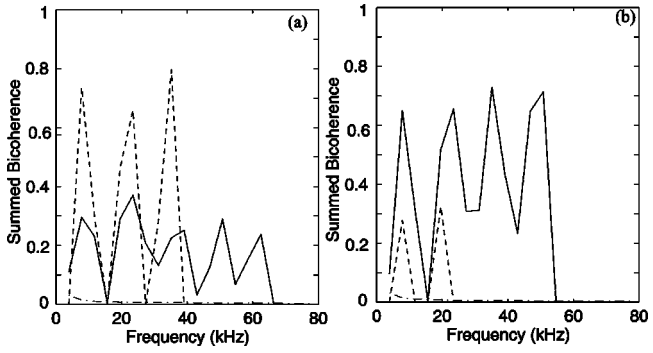

FIG. 6. Summed bicoherence for the time interval (2.04–3.06 ms) for the ion saturation current fluctuations, for the magnetic fields of 0.04 T (- - - -) and 1.00 T (——), at $r/a=0.85$ (a). The same for floating potential fluctuations (b). The dash–dotted line corresponds to the statistical error.

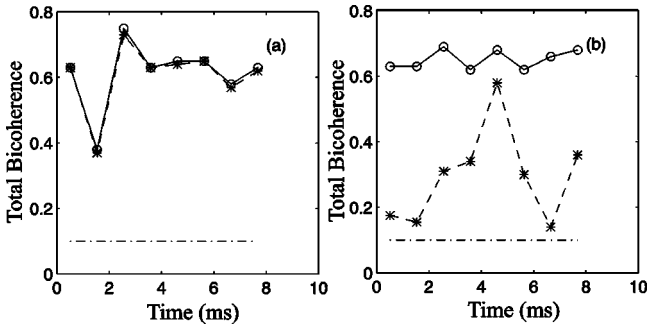

FIG. 7. Total bicoherence for ion saturation fluctuations as a function of time for the magnetic field of 0.04 T (*) and 1.00 T (○) (a). The same for plasma potential fluctuations (b). The dash–dotted line represents the maximum statistical error.

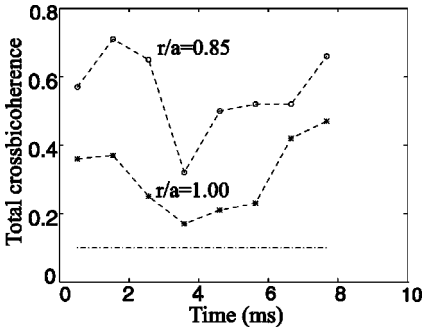

FIG. 9. Total cross-bicoherence as a function of time between potential and ion saturation current fluctuations for $r/a=0.85$ (○) or $r/a=1.00$ (*), for the magnetic field of 0.04 T. Dash–dotted line represents the maximum statistical error.

to frequencies higher than 40 kHz. Figures 8(c) and 8(d) are the contour plots of the bicoherence for the same fluctuations and intervals. Figure 8(d) clearly shows the influence of higher frequencies in the quadratic coupling. The main nonlinear coupling is essentially in the difference frequency regions. Furthermore, the observed quadratic coupling is much higher for $B_\varphi=1.00$ T. This result is consistent with the previously described amplitude grow of high frequency components, as the magnetic field is increased (Figs. 3 and 4). In other words, as the magnetic field increases the frequency spectra become broader due to energy transfer from low frequency (including the wave produced by the radio frequency oscillator) to high frequency oscillations.

The cross-bicoherence values calculated between potential and density fluctuations show higher values for plasma positions at the plasma edge. Figure 9 compares this total cross-bicoherence at $r/a=0.85$ (plasma edge) with the value calculated at $r/a=1.00$ (SOL), for a field of 0.04 T. During a discharge, we observed a pronounced time dependence in both positions but the quadratic coupling is lower in the SOL. The obtained results indicate relevant nonlinear coupling for these two kinds of fluctuations. For $B_\varphi=1.00$ T the cross-bicoherence values are as high as those shown in Fig. 9 but they are more uniform in space and time.

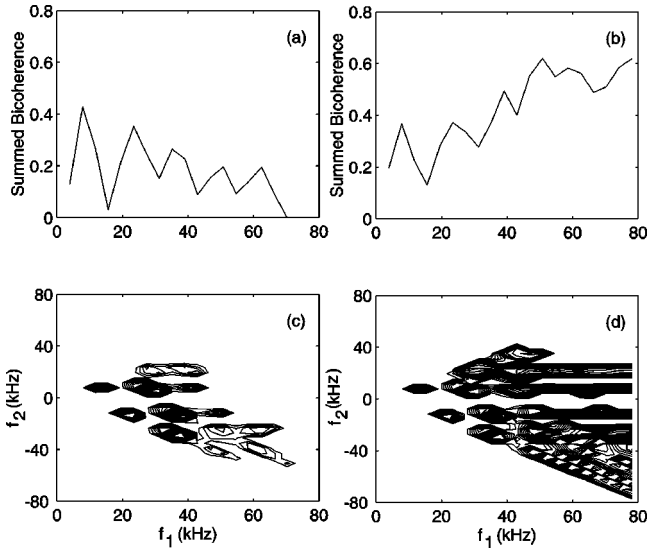

FIG. 8. Summed bicoherence for ion saturation current fluctuations at $r/a=1.00$, for time intervals (2.04–3.06 ms) (a); or (7.17–8.19 ms) (b), for the magnetic field of 1.00 T. Contour plots of the bicoherence for the same fluctuations, magnetic field and time intervals (c), (d).

IV. CONCLUSIONS

In this paper we describe a toroidal magnetoplasma (without plasma current) created by radio frequency waves and confined by a toroidal magnetic field. As expected, increasing this magnetic field produces a better confinement with pronounced radial gradients in the plasma parameter profiles. However, due to these gradients, the plasma is subject to several instabilities[1,7,8] among which the density gradient-driven instability.[4,11,12] As shown in other plasma confinement systems,[4–6,20] these drift wave instabilities may be responsible for the plasma edge turbulence observed in the plasma studied in this work.

We analyze the rising of turbulence in the investigated plasma by measuring density and potential fluctuation frequency spectra and bicoherence coefficients for two values of the toroidal magnetic field (0.04 T and 1.00 T).

In the regime of the low magnetic field, the plasma is practically uniform, fluctuation levels are smaller and spectra are significant only for predominant low frequency peaks concentrated around the frequency of the oscillator. Moreover, the nonlinear coupling is observed only for these coherent peaks.

In contrast, in the regime of a high magnetic field plasma parameter gradients are observed and a broad-band of high frequency fluctuations appears superposed to the previously mentioned low frequency components. In this regime, bicoherence analysis shows a large presence of nonlinear coupling between low and high frequency components, consistent with the observed amplitude grow of high frequency components as the magnetic field is increased. Therefore, as the magnetic field increases the frequency spectra become broader due to energy transfer from low frequency to high frequency oscillations, revealing the rising of turbulence.

The enhancement of the nonlinear coupling between fluctuating plasma potential and density observed for the highest magnetic field is predicted in the nonlinear electrostatic drift wave stability analysis presented in Ref. 21. Ac-

cording to this reference, this nonlinearly cross-coupling is more significant for the smaller radial decay coefficient λ_n observed, in our experiment, for the highest magnetic field.

The application of wavelet analysis revealed that the observed nonlinear coupling between low and high frequency components is not stationary. Indeed, as shown in Figs. 7 and 9, the nonlinear spectral characteristics change on a time scale smaller than the time discharge. These changes suggest that the plasma turbulence may be close to a threshold and that excursions across this threshold result in the intermittent variations in the level and nonlinear couplings of the turbulent fluctuations. In fact, this kind of intermittency was observed in another experiment for low-frequency electrostatic fluctuations with a plasma produced by a steady-state discharge in a magnetized toroidal plasma[6] without rotational transform.[22]

The simultaneous density gradient increment and the broadening of the frequency spectrum with the increasing magnetic field supports the presence of drift waves in the laboratory experiment presented here. Consequently, the development of plasma turbulence, with the increasing magnetic field, seems to be caused by a nonlinear wave–wave interaction process between the wave generated by the radio frequency oscillator and the drift waves associated to the continuous high frequency spectrum.

ACKNOWLEDGMENTS

The authors are indebted to Mr. Z. A. Brasílio and Dr. R. M. Castro for part of the computer programs used in the work and the TCABR team for the use of laboratory facilities.

This work was partially supported by Brazilian governmental agencies FAPESP (Fundação de Amparo à Pesquisa do Estado de São Paulo), CNPq (Conselho Nacional de Pesquisa) and CAPES (Fundação Coordenação de Aperfeiçoamento de Pessoal de Nível Superior).

[1] J. Wootton, B. A. Carreras, H. Matsumoto, K. McGuire, W. A. Peebles, Ch. P. Ritz, P. W. Terry, and S. J. Zweben, Phys. Fluids B **2**, 2879 (1990).
[2] F. Wagner and V. Stroh, Plasma Phys. Controlled Fusion **35**, 1321 (1993).
[3] Ch. P. Ritz, E. J. Powers, and R. D. Bengtson, Phys. Fluids B **1**, 153 (1989).
[4] U. Kauschke, G. Oelerich-Hill, and A. Piel, Phys. Fluids B **2**, 38 (1990).
[5] C. Riccardi, D. Xuantong, M. Salierno, L. Gamberale, and M. Fontanesi, Phys. Plasmas **4**, 3749 (1997).
[6] F. J. Øynes, O. M. Olsen, H. L. Pécseli, Å. Fredriksen, and K. Rypdal, Phys. Rev. E **57**, 2242 (1998).
[7] W. Horton, Phys. Rep. **192**, 1 (1990).
[8] J. D. Callen, Phys. Fluids B **4**, 2142 (1992).
[9] S. Santoso, E. J. Powers, R. D. Bengtson, and A. Ouroua, Rev. Sci. Instrum. **68**, 898 (1997).
[10] M. V. A. P. Heller, Z. A. Brasilio, I. L. Caldas, J. Stockel, and J. Petrzilka, Phys. Plasmas **6**, 846 (1999).
[11] D. Biskamp, *Nonlinear Magnetohydrodynamics* (Cambridge University Press, Cambridge, 1993).
[12] S. J. Camargo and H. Tasso, Phys. Fluids B **4**, 1199 (1992).
[13] A. G. Elfimov, R. O. Galvão, I. C. Nascimento, and G. Amarante Segundo, Plasma Phys. Controlled Fusion **39**, 1551 (1997).
[14] B. Ph. van Milligen, C. Hidalgo, E. Sánchez, M. A. Pedrosa, R. Balbín, I. García-Cortés, and G. R. Tynan, Rev. Sci. Instrum. **68**, 967 (1997).
[15] C. Chui, *An Introduction to Wavelets* (Academic, San Diego, CA, 1992).
[16] B. Ph. van Milligen, E. Sánchez, T. Estrada, C. Hidalgo, B. Brañas, B. Carreras, and L. García, Phys. Plasmas **2**, 3017 (1995).
[17] T. Levinson, J. M. Beall, E. J. Powers, and R. D. Bengtson, Nucl. Fusion **24**, 527 (1984).
[18] D. C. Robinson, ''Confinement and electrostatic and electromagnetic fluctuations,'' in *Turbulence and Anomalous Transport in Magnetized Plasmas*, edited by D. Gresillon and M. A. Dubois (Editions de Physique, France, 1986), pp. 21–52.
[19] R. Jha, S. K. Mattoo, and Y. C. Saxena, Phys. Plasmas **4**, 2982 (1997).
[20] G. Prasad, D. Bora, and Y. C. Saxena, Phys. Plasmas **1**, 1832 (1994).
[21] S. J. Camargo, D. Biskamp, and B. D. Scott, Phys. Plasmas **2**, 48 (1995).
[22] H. Tasso, B. J. Green, and H. P. Zeerhfeld, Phys. Fluids **12**, 2444 (1969).